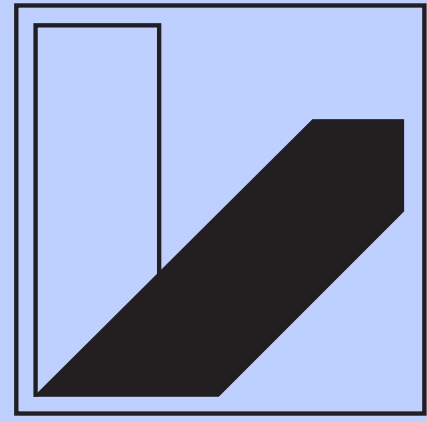


# Modeling of Electrodes for Lithium-Ion Batteries

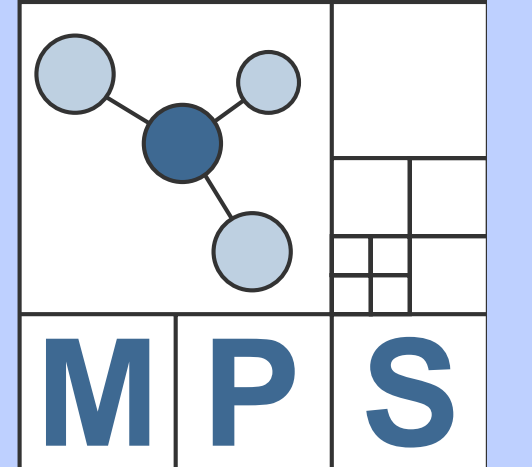


UNIVERSITÄT  
BAYREUTH

(LiFePO<sub>4</sub>), a phasefield approach

H. Federmann, M. Fleck and H. Emmerich

Materials & Process Simulation (MPS), University of Bayreuth, Germany



## 1. What is the reason to choose LiFePO<sub>4</sub> as cathode material?

Olivine LiFePO<sub>4</sub> has been considered as the most promising cathode candidate for the next generation large scale lithium-ion battery used for high energy consuming applications. The advantages are: a theoretical capacity of 170 mAh/g, low toxicity, long cycle ability and high safety.[4]

## 2. Material properties

Phase behavior and phase transition kinetics at electrode level directly affect numerous battery performance metrics. The electrochemically induced phase transformation is fundamentally not different from other types of phase transitions. Hence, the same thermodynamic principles could be used. [1].

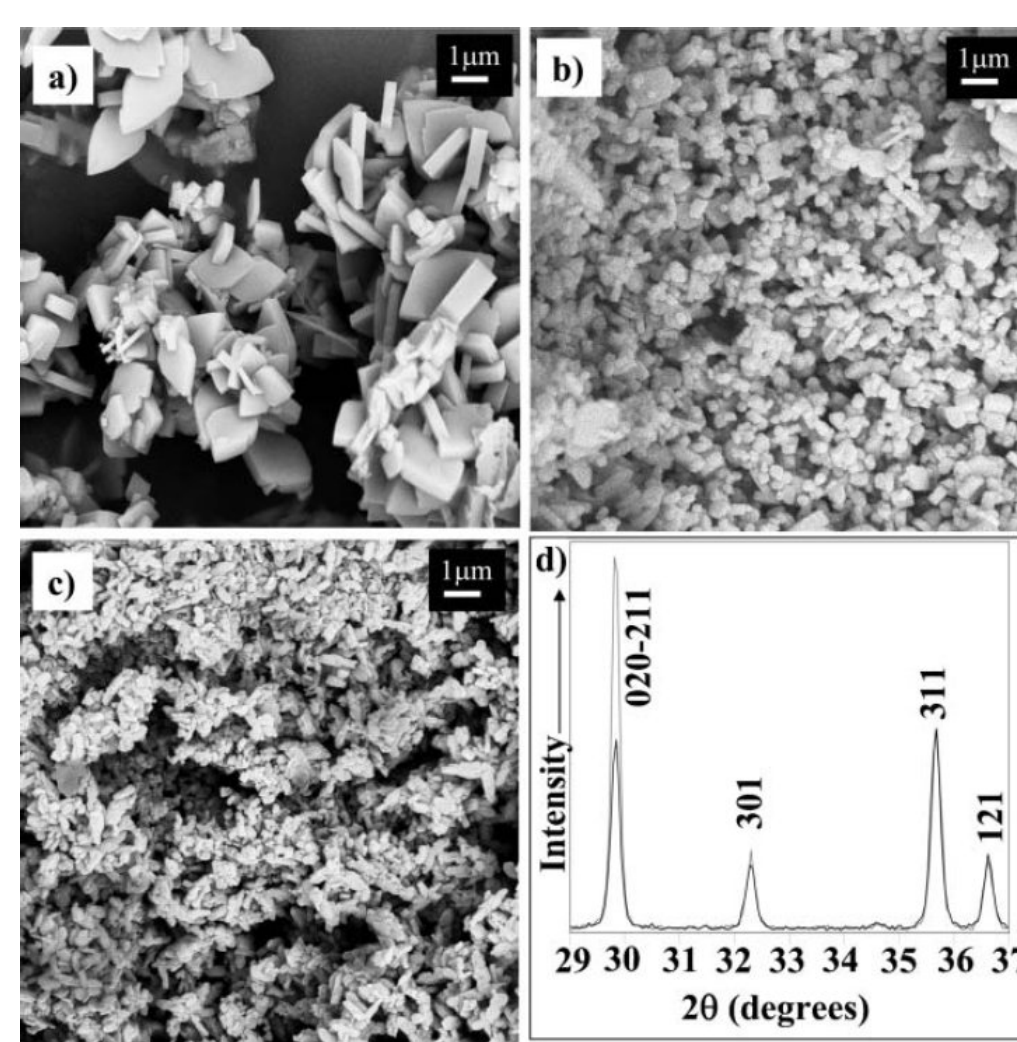


Figure 1: SEM micrographs of carbon free LiFePO<sub>4</sub> crystallized at different concentrations and temperatures (facet shape) [3].

### 2.1 Olivine structure

LiFePO<sub>4</sub> has an orthorhombic olivine structure with experimental lattice parameters  $a = [100] = 10.3375 \text{ \AA}$ ,  $b = [010] = 6.0112 \text{ \AA}$  and  $c = [001] = 4.6950 \text{ \AA}$ . The lattice consists of a distorted hexagonal close-packed framework containing Fe<sup>2+</sup> ions which are sixfold coordinated by oxygen atoms forming layers of edge-sharing octahedra. The individual layers are separated by PO<sub>4</sub> tetrahedra. Lithium can be electrochemically removed from the crystal without changing the olivine topology. The experimental lattice parameters of delithiated FePO<sub>4</sub> are  $a = [100] = 9.7599 \text{ \AA}$ ,  $b = [010] = 5.7519 \text{ \AA}$  and  $c = [001] = 4.7560 \text{ \AA}$  [5].

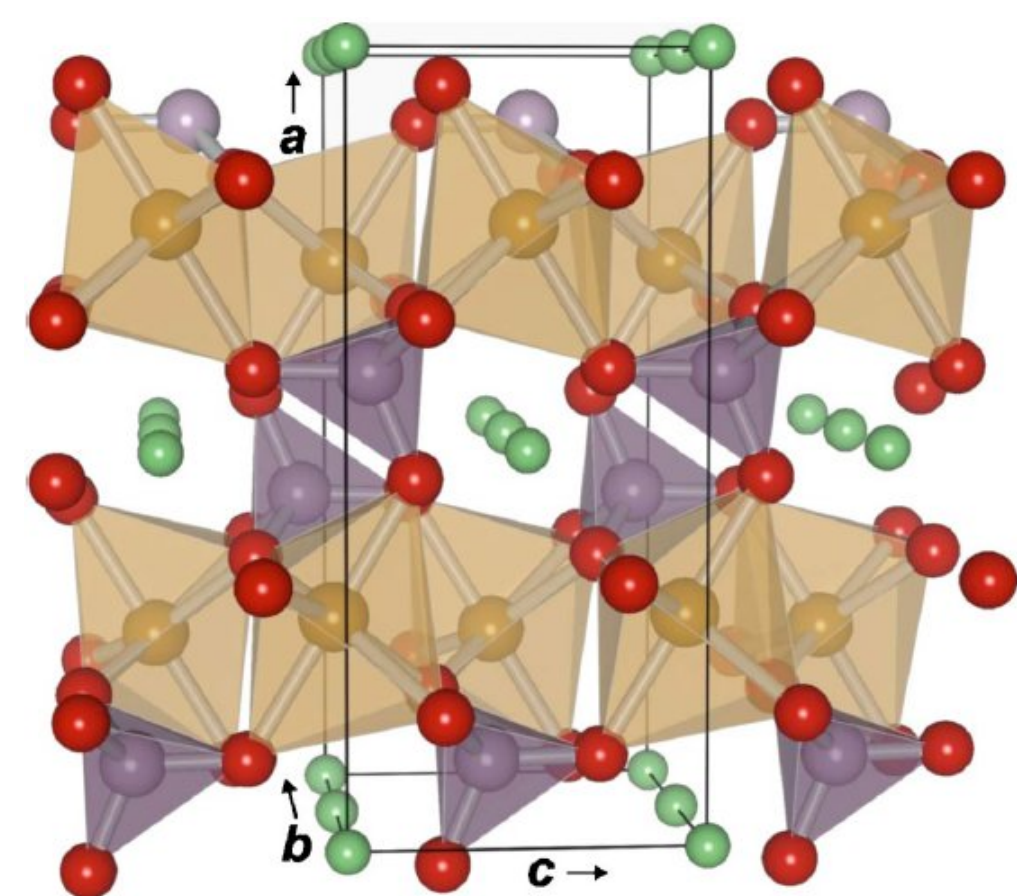


Figure 2: LiFePO<sub>4</sub> olivine structure: Fe octahedra yellow, P tetrahedra purple, Li atoms green and O atoms red [5].

### 2.2 Charge and discharge of a single particle

In this material, the electric energy is stored by incorporating Li<sup>+</sup> ions into the olivine FePO<sub>4</sub> crystal. Therefore, the power capability of a lithium battery will depend critically on the rate at which the Li<sup>+</sup> and e<sup>-</sup> can migrate through the cathode material system.[6]

The LiFePO<sub>4</sub> electrode -discharging and -charging process is enabled by Li<sup>+</sup> and e<sup>-</sup> diffusion into (out of) the active cathode particles. The diffusion kinetics of Li and electrons are fundamental to the behavior of the material during electrochemical cycling. First-principles calculations have shown that Li<sup>+</sup> diffusion in the bulk FePO<sub>4</sub> crystal is highly anisotropic. Li<sup>+</sup> transport is essentially constrained to 1D channels in the [0 1 0] direction [7], see Fig. 3.

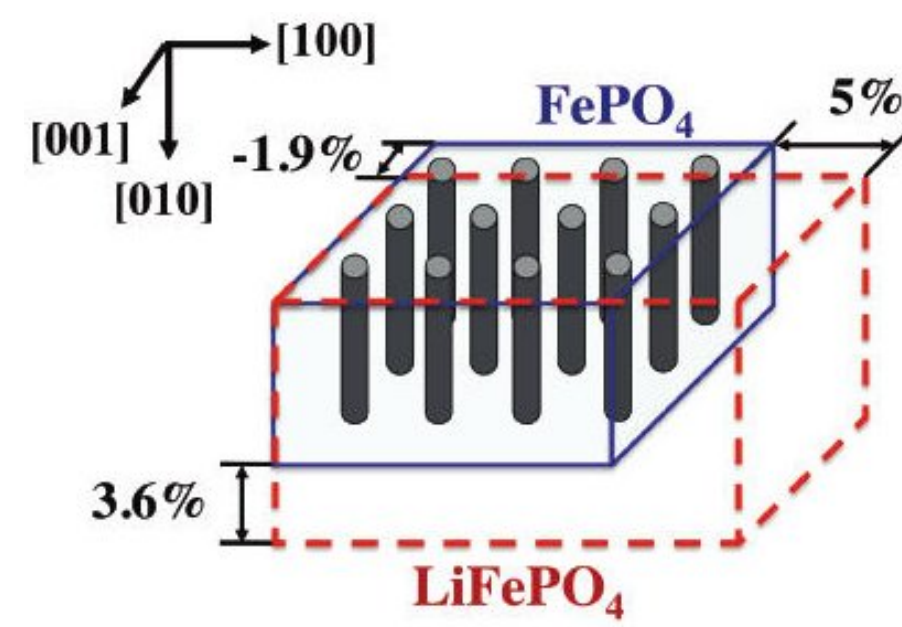


Figure 3: 1-D Li<sup>+</sup> diffusion channels along [010] and anisotropic misfit strain between FePO<sub>4</sub> and LiFePO<sub>4</sub> [2].

A schematic views of the interfacial region between LiFePO<sub>4</sub> and FePO<sub>4</sub> phases is shown in Fig.4: (a) indicates the diffuse interface; (b) and (c) show the interface evolution during delithiation and lithiation, respectively. Small vertical arrows indicates the extraction/ insertion of (Li<sup>+</sup>, e<sup>-</sup>) pairs into the diffusion channels.

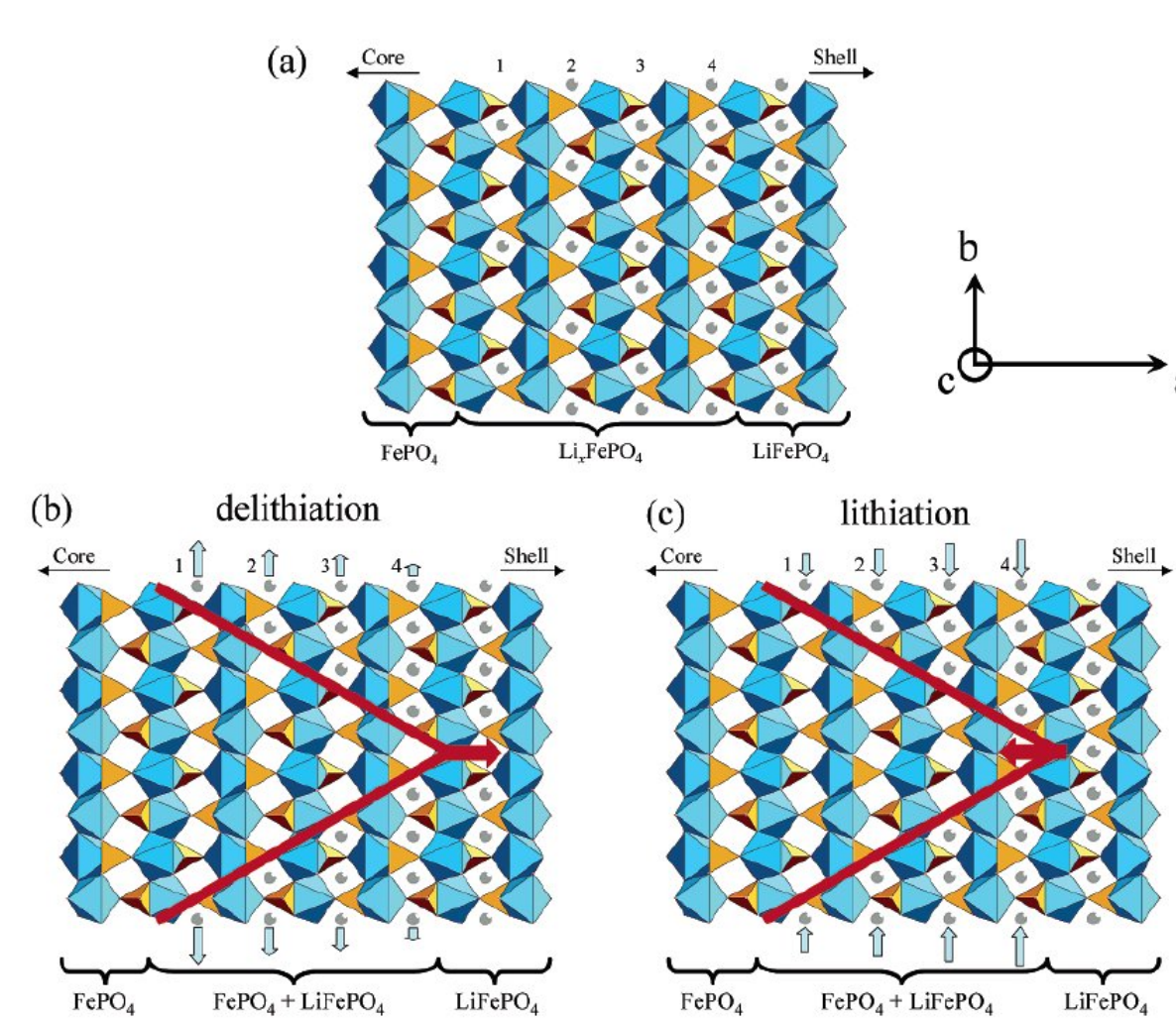


Figure 4: Lithium deinsertion/insertion process [8].

## 3. Phase field modeling

We present a general continuum framework to describe intercalation dynamics in rechargeable battery materials. Our model can be adapted to arbitrary intercalation compounds depending on the physical constants and the chemical driving force.

- The phasefield  $\phi(\vec{x}, t)$  draws a distinction for two different phases:  $\phi = 1$  denotes the lithium rich phase (LFP) and  $\phi = 0$  for the lithium poor phase (FP). The total free energy of the system is given by

$$F[\phi(\vec{x}, t)] = \int_V \{f_{int}(\phi, \nabla\phi) + f_{chem}(c, \phi) + f_{el}(\epsilon_{ik}, \phi)\} dV. \quad (1)$$

- The interfacial free energy is given by

$$f_{int}(\phi, \nabla\phi) = \frac{3\gamma\xi}{2}(\nabla\phi)^2 + \frac{6\gamma}{\xi}g(\phi), \quad (2)$$

where  $g(\phi) = \phi^2(1-\phi)^2$  is the double well potential.  $\gamma$  is the surface energy and  $\xi$  is the interface width. Hence the free energy has two local minima at  $\phi = 1$  and  $\phi = 0$ .

- The chemical free energy is given by

$$f_{chem} = \frac{X}{2} \left( c - h(\phi)c_{eq}^{LFP} - (1-h(\phi))c_{eq}^{FP} \right)^2 + p_n(c), \quad (3)$$

with the interpolation function  $h(\phi) = \phi^2(3-2\phi)$ . The polynom contribution  $p_n(c)$  takes into account the energy dependence on the different concentrations.  $X$  represents a thermodynamic factor.

- The elastic free energy can be written as

$$f_{el}(\epsilon_{ik}, \phi) = \frac{1}{2} \bar{\epsilon}_{ik} \bar{C}_{iklm} \bar{\epsilon}_{lm} \quad (4)$$

$$\bar{C}_{iklm} = h(\phi)C_{iklm}^{LFP} + (1-h(\phi))C_{iklm}^{FP} \quad (5)$$

$$\bar{\epsilon}_{ik} = \epsilon_{ik} - \epsilon_{ik}^0 h(\phi). \quad (6)$$

The unstressed matrix is set as the reference so that its eigenstrain vanishes.

- The kinetic equations are derived from the free energy functional. The evolution for the lithium concentration  $c$  is given by the following diffusion equation (anisotropic):

$$\frac{\partial c}{\partial t} = \nabla \cdot (\mathbf{D} \nabla \mu) + (c_{eq}^{LFP} - c_{eq}^{FP}) h'(\phi) \frac{\partial \phi}{\partial t}. \quad (7)$$

The chemical potential could be calculated from  $c$  by

$$\mu = \frac{\delta F}{\delta c} = X \{ c - h(\phi)c_{eq}^{LFP} - (1-h(\phi))c_{eq}^{FP} \} + p_n'(c). \quad (8)$$

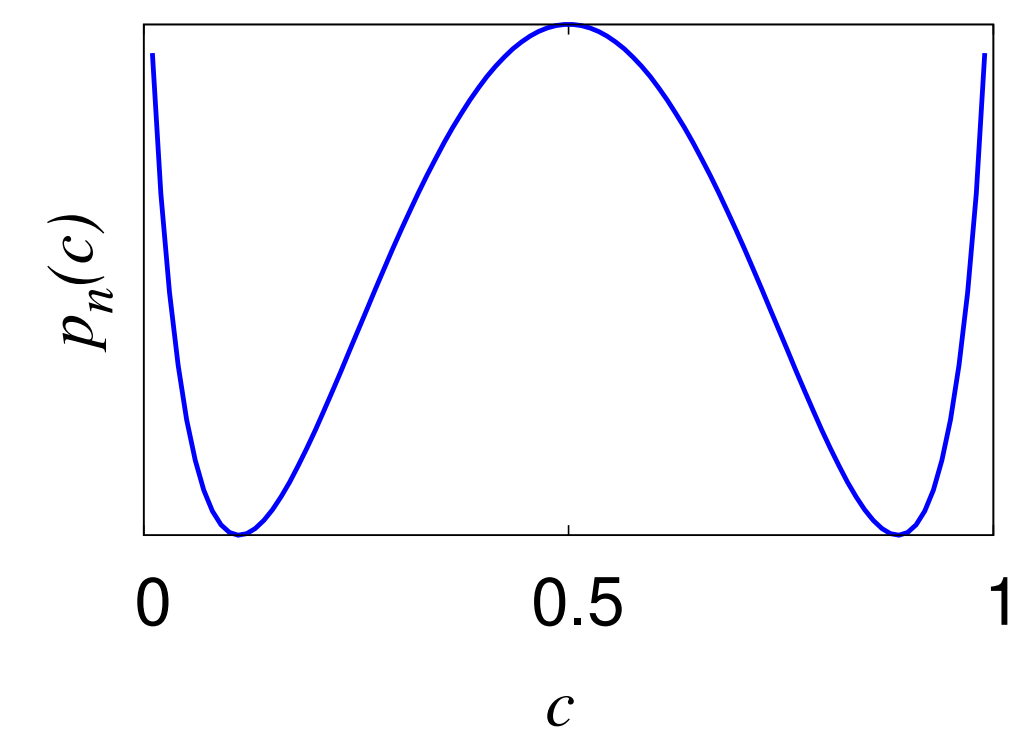


Figure 5:  $p_n = \frac{3}{2} \{ \ln(1-c)(1-c) + c \ln(c) \} + 1 - 4 \left( \frac{1}{2} - c \right)^2$

A dissipative Allen-Cahn equation describes the evolution of the phase field

$$\frac{1}{M} \frac{\partial \phi}{\partial t} = - \frac{1}{3\gamma\xi} \frac{\delta F}{\delta \phi} = \nabla^2 \phi - \frac{2}{\xi^2} g'(\phi) - \frac{1}{3\gamma\xi} \frac{\partial f_{chem}}{\partial \phi} - \frac{\partial f_{el}}{\partial \phi} \quad (9)$$

where  $M$  is the kinetic coefficient. The strain and stress for the mechanical equilibrium are defined by

$$\sigma_{ik} = \frac{\partial f_{el}}{\partial \epsilon_{ik}}, \quad 0 = \frac{\partial \sigma_{ik}}{\partial x_k}, \quad (11)$$

where  $\epsilon_{ik} = \frac{1}{2} \{ \partial_i u_k + \partial_k u_i \}$ .

## 4. Simulation (without elastic effects)

The lithium intercalation process was simulated for a rectangular particle. A overpotential is applied to the top and the bottom of the system to provide driving force for Li insertion into an initially delithiated particle. The FP  $\rightarrow$  LFP phase transition occurs by nucleation in the particle corners being the most favored nucleation sites. A supercritical LFP nucleus is thus placed at a particle corner at the beginning of the simulation to initiate LFP growth. The progressive movement of the phase boundary was limited by diffusion. A steady state velocity is arising and a stationary interface profile is obtained. The shape of the front was caused by local lithium depletion.

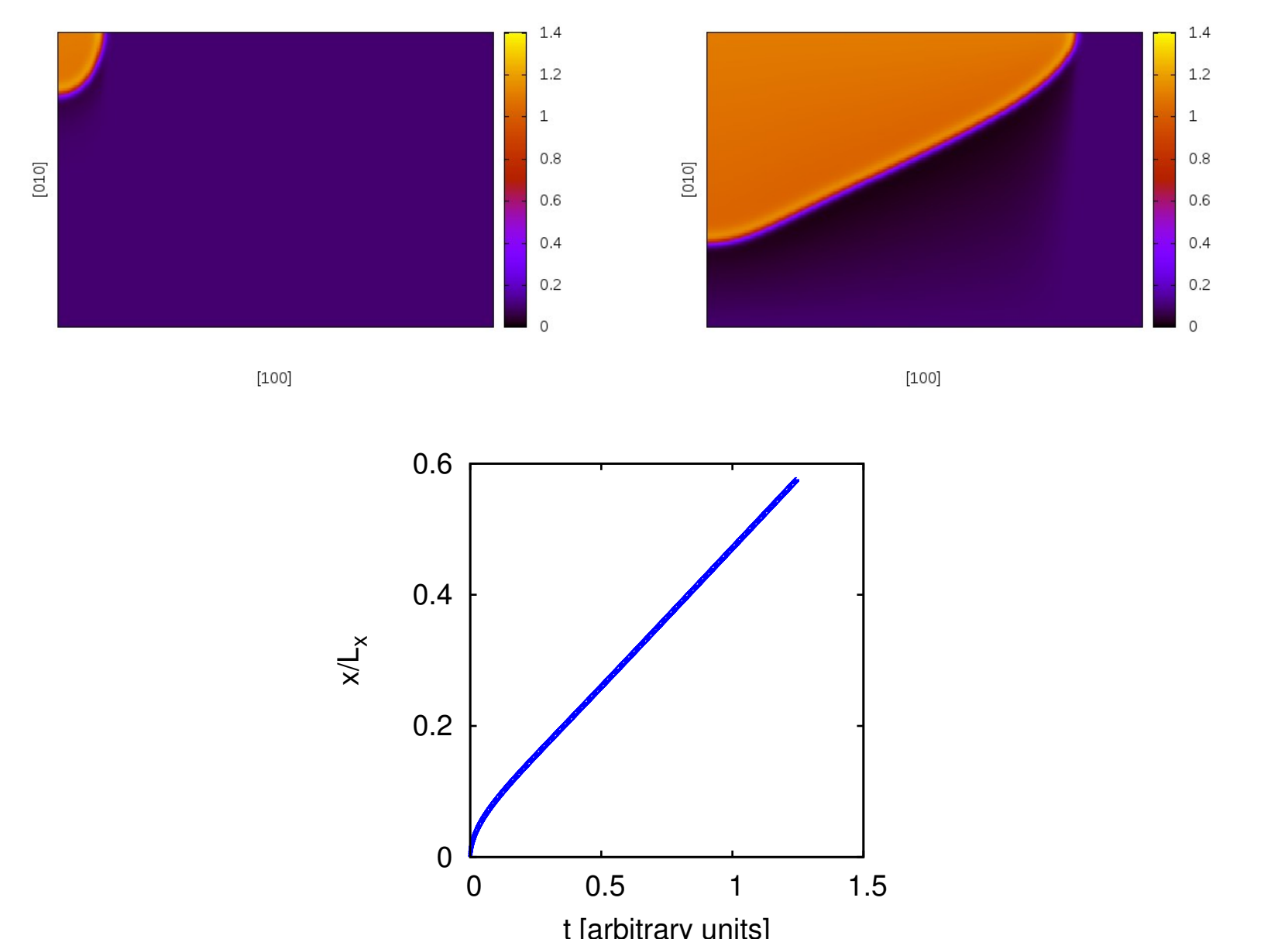


Figure 6: Particle discretized on a 400 x 200 mesh. The colours are representing the Li<sup>+</sup> concentration. Snapshots: start condition, step 216000 and below the evolution of phase boundary with time.

## References

- [1] Ming Tang, W. Craig Carter and Yet-Ming Chiang, , Annu. Rev. Mater. Res. 40:501-29, 2010.
- [2] Ming Tang, James F. Belak and Milo R. Dorr, ,J. Phys. Chem. C, 115, 4922-4926, 2011.
- [3] B. Ellis, Wang Hay Kan, W. R. M. Makahnouk and L. F. Nazar, J. Mater. Chem., 17, 3248-3254, 2010.
- [4] Yonggang Wang, Ping He and Haoshen Zhou, Energy Environ. Sci., 4, 805-817, 2011.
- [5] T. Maxisch, G. Ceder, Phys. Rev. B 73, 174112, 2006.
- [6] B. Kang and G. Ceder, NATURE , Vol 458, 12 March 2009.
- [7] G. K. Singh, G. Ceder and M. Z. Bazant, Electrochimica Acta, 53, 7599-7613, 2008.
- [8] L. Laffont, C. Delacourt, P. Gibot, M. Y. Wu, P. Kooyman, C. Masquelier and j. M. Tarascon, , Chem. Mater., 18, 5520-5529, 2006.